Influence of different functionalization methods of multi-walled carbon nanotubes on the properties of poly(L-lactide) based nanocomposites

Nevena Vukić[1], Ivan S Ristić[1], Milena Marinović-Cincović[2], Radmila Radičević[1], Branka Pilić[1], Suzana Cakić[3], and Jaroslava Budinski-Simendić[1]

[1]*University of Novi Sad, Faculty of Technology Novi Sad,, Novi Sad, Serbia*
[2]*Vinča Institute of Nuclear Science, University of Belgrade, Serbia*
[3]*University of Niš, Faculty of Technology, Leskovac, Serbia*

Abstract

This paper presents influence of the type of carbon nanotube functionalization on properties of poly(L-lactide) (PLLA) based nanocomposite materials. For this purpose surface modifications of multi-walled carbon nanotubes (MWCNTs) were performed by chemical and irradiation techniques, while thermo gravimetric analysis, UV-Visible and Fourier-transform infrared (FT-IR) spectroscopies confirmed successful covalent functionalization. Series of PLLA bionanocomposites with different contents of functionalized MWCNTs (0.7; 1.6; 2.1 wt%), were synthesized *via* ring-opening solution polymerisation of L-lactide. FT-IR analysis confirmed that grafting of L-lactide, under controlled condition, is possible to perform starting from the surface of functionalized MWCNTs. From differential scanning calorimetry results it was concluded that even low contents of chemically and irradiation functionalized MWCNTs had a significant effect on thermal properties of the prepared nanocomposites, raising the values of melting and glass transition temperatures. Thermogravimetric analysis (TGA) has shown that the degradation onset temperature for composites with chemically functionalized MWCNTs, was much higher than that for the neat poly(L-lactide) sample and composites with irradiation functionalized MWCNTs. Morphology studies by scanning electron microscopy (SEM) and transmission electron microscopy (TEM) indicated that poly(L-lactide) covered surfaces and separated functionalized MWCNTs. Good dispersion of carbon nanotubes in polymer matrix enabled conductivity of synthesized materials, as determined by conductivity tests.

Keywords: nanocomposites; carbon nanotube functionalization; poly(L-lactide); thermal properties

Dostupno na Internetu sa adrese časopisa: http://www.ache.org.rs/HI/

SCIENTIFIC PAPER

UDK: 678.017+66.017:620.3:536.4

Hem. Ind. **73 (3)** 183-196 (2019)

1. INTRODUCTION

Since the discovery of carbon nanotubes (CNTs) in 1991 by Iijima [1], they have received a lot of attention due to many potential applications that they might have. By exhibiting unique properties (electric, thermal, mechanical, *etc.*), CNTs hold promise for development of fundamentally new materials, especially polymer nanocomposites [2,3]. However, excellent properties of CNTs do not guarantee superior properties of resulting composites due to strong influences of various factors such as quality of CNTs dispersion as well as the interfacial adhesion between CNTs and the polymer matrix [4]. CNTs are known to form aggregates during compounding and therefore various techniques have been used to overcome this problem such as the use of sonication or mechanical mixing during fabrication of the nanocomposite. The most effective way to resolve this problem is surface functionalization of CNTs [5]. Types of CNT modifications are basically divided into two categories: one that involves the π-conjugated skeleton of CNTs in chemical reactions with various reagents, and the second in which chemical groups are introduced at the CNT surface thus providing adsorption of various molecules through

Corresponding author: Nevena Vukić, Department of Materials Engineering, Faculty of Technology Novi Sad, University of Novi Sad, Blvd cara Lazara 1, 21000 Novi Sad, Serbia; Phone: +381214853760
E-mail: nevenavukic@uns.ac.rs
Paper received: 2 April 2019
Paper accepted: 26 June 2019
https://doi.org/10.2298/HEMIND190402016V

non-covalent interactions. Covalent functionalization of CNTs can improve solubility as well as dispersibility in solvents and polymers. In general, functional groups such as –COOH or –OH can be created on CNTs during oxidation by oxygen, air, aqueous hydrogen peroxide, concentrated sulphuric acid, nitric acid or acid mixtures [6,7]. Also, this type of CNT functionalization can be achieved by using high energy irradiation techniques [8]. The extent of functionality induced by –COOH and –OH groups depends on the oxidation procedures and oxidizing agents [9]. The presence of these groups on the nanotube surface supports attachment of organic [10,11] or inorganic materials, which is important for solubilisation of nanotubes. Functionalization of CNTs by polymer grafting is particularly significant for processing of advanced composites [12,13] and can be formed by covalent attachment of highly soluble linear polymers onto the surface of nanotubes [14,15]. According to the "grafting from" approach, the polymer is bound to the CNT surface by *in-situ* polymerisation of monomers in the presence of reactive CNTs or CNT supported initiators. The main advantage of this procedure is that polymer/CNTs composites can be prepared at high grafting densities. This approach has been successfully used to graft many polymers onto CNTs *via* radical, cationic, anionic, ring-opening, and condensation polymerisations [16–21].

In the context of growing global environmental and social concerns, composite materials based on biopolymers are gaining grounds as the materials for the future [22]. Poly(lactide) (PLA) based nanocomposites represent a new class of nanosized biobased, biodegradable and biocompatible materials, exhibiting unique properties and functionalities. Bionanocomposites based on poly(lactide) and carbon nanotubes are currently of great interest for potential use in an extensive range of different applications [23,24]. Due to the existence of a chiral carbon in lactic acid, the repeating unit of PLA can have two different configurations (D or L) and the relative amount and distribution of these stereoisomers influence properties of this polymer material [25]. Recently, poly(L-lactide) has attracted increasing attention, despite some disadvantages that limit its more extensive employment. These disadvantages can be resolved by introducing suitable nanofillers. CNTs offer possibilities to combine PLLA properties with several unique features of these nanotubes. Due to the fact that the electric field is known to stimulate healing of various tissues, while PLLA is used as a biodegradable matrix in orthopaedic materials [26], this type of composites can be potentially used as electrical stimulation implants. Besides, PLLA based conductive nanocomposites can be possibly used as an antistatic coating material or for electromagnetic shielding [27]. Several studies have shown that addition of CNTs is beneficial for improving characteristics of PLA composites, especially in terms of thermal and electrical properties [23,26,28]. In this study, we have prepared a series of PLLA-multi-walled carbon nanotube (PLLA-MWCNT) bionanocomposites by direct ring-opening polymerisation of L-lactide from the surface of functionalized multi-walled carbon nanotubes (f-MWCNTs). MWCNTs were functionalized by chemical and radiation techniques. The influence of functionalization type on properties of the obtained PLLA based nanocomposites was investigated in details by thermal (differential scanning calorimetry, thermogravimetric analysis) and morphological studies (atomic force microscopy (AFM), scanning electron microscopy (SEM) and transmission electron microscopy, (TEM)). Also, synthesized biocomposites with the addition of differently functionalized MWCNTs were analysed regarding conductivity.

2. EXPERIMENTAL

2. 1. Materials

Monomer *(3S)-cis*-3,6-dimethyl-1,4-dioxane-2,5-dione (L-lactide) (purity of 98 %) and the catalyst trifluoromethanesulfonic acid (purity of 99%, density 1.696 g cm^{-3} at 25 °C) were supplied from Sigma-Aldrich (Germany). Pristine multi-walled carbon nanotubes (diameter of 13 nm, length of 1 μm and purity of 95 %) were supplied by Bayer MaterialScience (Germany). Nitric acid (concentration 60 wt%) and sulphuric acid (concentration 95 wt%) were supplied by Zorka Pharm (Serbia). Dichloromethane was purchased from Sigma-Aldrich (Germany) and dried by distillation before the use. The monomer L-lactide was recrystallized from methanol at least three times to remove traces of impurities before polymerisation.

2 .2. Covalent functionalization of carbon nanotubes

Functionalization of pristine MWCNTs was carried out by two different methods (oxidation by a mixture of strong acids and an irradiation technique). In the first one, a 250 ml flask was charged with 1.5 g of crude MWCNTs and a

mixture of HNO_3 and H_2SO_4, 100 ml (1/2 v/v), followed by sonication in a bath for 6 hours at room temperature. The obtained chemically functionalized nanotubes (chf-MWCNT) were washed with deionized water till the pH 7.0, and then dried under vacuum for 12 h at 60 °C. In the second method, functionalized MWCNTs were obtained from pristine MWCNTs by using γ irradiation as it was described in previous reports [8,29]. In brief, MWCNTs were sonicated in water, then were irradiated by using a gamma ray flux from ^{60}Co nuclide with the photon energy of 1.3 MeV at the Radiation sterilization unit (Vinča Institute of Nuclear Sciences, University of Belgrade, Serbia) with the dose rate of 10 kGy h^{-1}. The Radiation Unit has been described in more detail elsewhere [30], the facility core is Co-60 gamma irradiator with wet storage working in a batch mode (CEA, France). The samples were exposed to the γ irradiation dose of 100 kGy. After irradiation treatments, the obtained powdered samples (γ-MWCNT) were air-dried at room temperature.

2. 3. Preparation of f-MWCNT-PLLA nanocomposites

To prepare a series of f-MWCNT-PLLA nanocomposites, ring-opening polymerisation of L-lactide was carried out in the presence of various concentrations of f-MWCNTs, used as an initiator. Compositions used for sample preparations are summarized in Table 1. Solution polymerisation, in dichloromethane, was performed in a glass reactor at room temperature for 6 h with magnetic stirring of 300 rpm. Trifluoromethanesulfonic acid was used as a catalyst, in the ratio of 0.1 wt% to the amount of the L-lactide monomer. The obtained nanocomposites were dried in a vacuum oven at 50 °C for 12 h.

Table 1. *Formulations of synthesized materials*

Sample name	L-lactide	chf-MWCNTs	γ-MWCNTs
	Content, wt%		
PLLA	100	/	/
chf-MWCNT-PLLA-0.7	99.3	0.7	/
chf-MWCNT-PLLA-1.6	98.4	1.6	/
chf-MWCNT-PLLA-2.1	97.9	2.1	/
γ-MWCNT-PLLA-0.7	99.3	/	0.7
γ-MWCNT-PLLA-1.6	98.4	/	1.6
γ-MWCNT-PLLA-2.1	97.9	/	2.1

2. 3. Characterization of MWCNTs and f-MWCNT-PLLA nanocomposites

UV-Vis spectra of pristine and functionalized multi-walled carbon nanotubes were taken in the range from 190 nm to 700 nm using a UV–Vis spectrophotometer (VARIAN Cary-100 Conc. Spectrophotometer, Varian, USA) at 30 °C. For the analysis, water dispersions (2 wt%) of carbon nanotubes were prepared.

Molecular structures of MWCNTs and prepared nanocomposite materials were characterized by Fourier-transform infrared (FT-IR) spectroscopy. FT-IR spectra were recorded by a Michaelson Bomem MB-series spectrophotometer (Bomem Inc, Canada) in the transmission mode at the wavelength range of 400–4000 cm^{-1} with the resolution of 2 cm^{-1}. Measurements were carried out using the KBr pellet (1 mg samples/100 mg of KBr) technique.

Thermal properties of the samples were investigated by differential scanning calorimetry using a DSC Q20 instrument (TA Instruments, USA). Hermetically sealed aluminium pans containing 3-5 mg of a sample were prepared. All samples were melted at 180 °C, to ensure complete melting and resetting the thermal history, and rapidly cooled to 20 °C. The non-isothermal measurement was scanned from 20 to 180 °C with a heating rate of 10 °C min^{-1}.

Crystallization degree (X_c) was estimated according to the following equation:

$$X_c\,/\,\% = \frac{\Delta H_m}{\Delta H_m^{\,0} wt_{PLA}} 100 \qquad (1)$$

where ΔH_m refers to the enthalpy of melting of the examined sample, ΔH_m^0 refers to the enthalpy value of 100 % crystalline PLA, which is 93 J g^{-1} and wt_{PLA} refers to the weight ratio of PLA in PLA-MWCNT composites [31].

Thermogravimetric analyses (TGA) were performed on a Setaram Setsys Evolution-1750 instrument (Setaram, France). Samples of approximately 10 mg were heated from 25 to 1000 °C at the heating rate of 10 °C min^{-1} in argon atmosphere with the gas flow rate of 20 cm^3 min^{-1}.

Morphology of nanocomposites was characterized by using a scanning electron microscope (JEOL JSM-6460, JEOL, Japan), transmission electron microscope (JEOL JEM-2100 LaB6) with accelerating voltage of 200 kV equipped with the high-resolution (HR) style objective-lens pole piece, (JEOL, Japan) and an atomic force microscope (Quesant 250 tabletop microscope, Quesant, USA), operating in a tapping mode in air at room temperature. Specimens for SEM images were prepared by fracturing the amorphous nanocomposites in a liquid nitrogen bath and coating the surfaces with a gold layer. For AFM measurements all samples were deposited using standard spin coating equipment at 4000 rpm. Standard silicon tips with the constant force of 40 N m^{-1} were used.

Conductivity of nanocomposites was analysed by measuring the sheet resistivity of samples [32]. The sheet resistivity of MWCNT-PLLA nanocomposites was taken by a four-point probe device (Jandel RM 3000 Universal probe, Jandel, United Kingdom) taking into account five different places on the composite surface and the obtained values were averaged. All measurements were performed at room temperature.

3. RESULTS AND DISCUSSION

3. 1. Characterization of functionalized carbon nanotubes

UV-Vis spectra of pristine (MWCNT), chemically functionalized (chf-MWCNT) and irradiated (γ-MWCNT) carbon nanotubes are presented in Figure 1. Pristine MWCNTs have shown an absorption peak at 282 nm, which was attributed to π-π* electron transition in MWCNTs. Compared with spectra of pristine carbon nanotubes it can be observed that this peak observed at 282 nm (π - π*) blue shifted to 276 nm and 265 nm for γ-MWCNTs and chf-MWCNTs, respectively. The possible reason is as follows: the energy of π* (π antibonding orbit) in MWCNTs is increased because of the π-π stacking interaction between the MWCNTs and the newly formed functional groups (carboxyl and/or hydroxyl) resulting in the increase in the energy necessary for π-π* electron transition. Thus, the characteristic peak assigned to this electron transition blue shifted for both applied functionalization methods [33–35]. This peak is more intense for chemically functionalized MWCNTs in comparison to irradiated ones, due to oxidation of chf-MWCNTs in acids, which leads to a higher number of carboxyl groups on the nanotube surface.

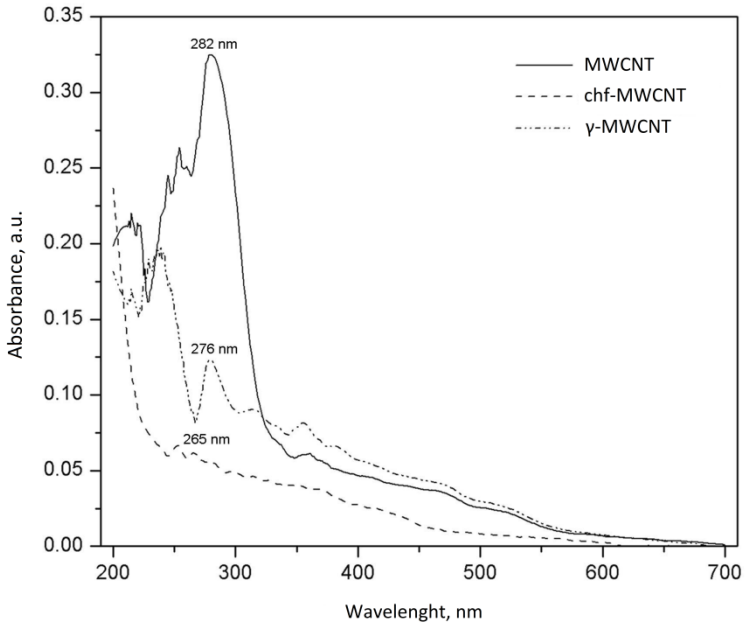

Fig. 1. UV-Vis spectra of pristine (MWCNT), chemically functionalized (chf-MWCNT) and irradiated (γ-MWCNT) carbon nanotubes

FT-IR spectra of pristine and functionalized nanotubes are shown in Figure 2. In the spectrum of pristine MWCNTs signal is almost absent except for a small peak corresponding to the stretching vibrations of C-C bonds, while with functionalization a number of new peaks appear in the spectra of f-MWCNTs. The FT-IR spectra of f-MWCNTs show medium and weak line at 3749 cm^{-1}, which indicates the presence of unbound or free hydroxyl group (–OH). The peak at 3433 cm^{-1} can be assigned to the stretching vibrations of O–H bonds in carboxyl groups (O=C–(−OH) and C–OH). In the spectra of the functionalized nanotubes, the band at around 1708 cm^{-1} corresponds to the stretching vibrations of C=O bonds. The peak at 1360 cm^{-1} is assigned to δ_{C-O} vibrations (from C(=O)-OH). The band at 1166 cm^{-1} is assigned to vibrations of C-O bond from the secondary hydroxyl functional groups attached to sidewalls of the nanotubes.

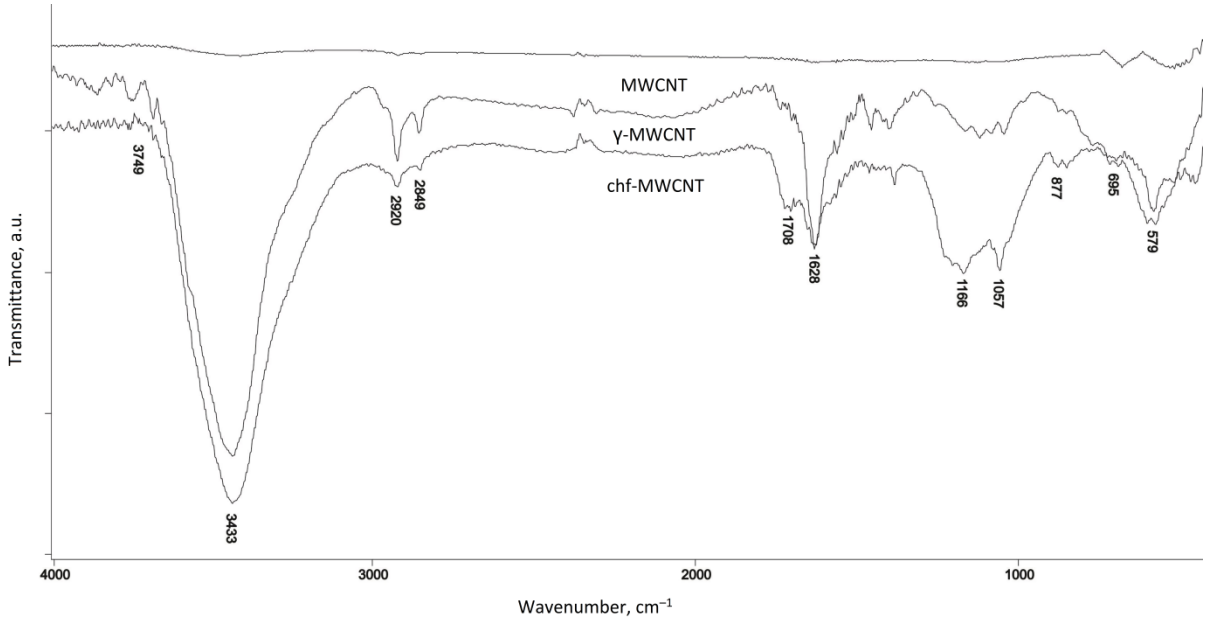

Fig. 2. FT-IR spectra of pristine, irradiation (γ-MWCNT) and chemically (chf-MWCNT) functionalized carbon nanotubes

Thermogravimetric analysis provides useful information on the extent of covalent functionalization because the groups (-COOH and -OH) attached to the sidewalls of MWCNTs are thermally unstable and degrade before the onset of the MWCNT weight loss [36]. For pristine MWCNTs, the mass loss was not observed in the temperature range 25 – 1000 °C and thus the residue content at 1000 °C was 96.5 wt% (Fig. 3).

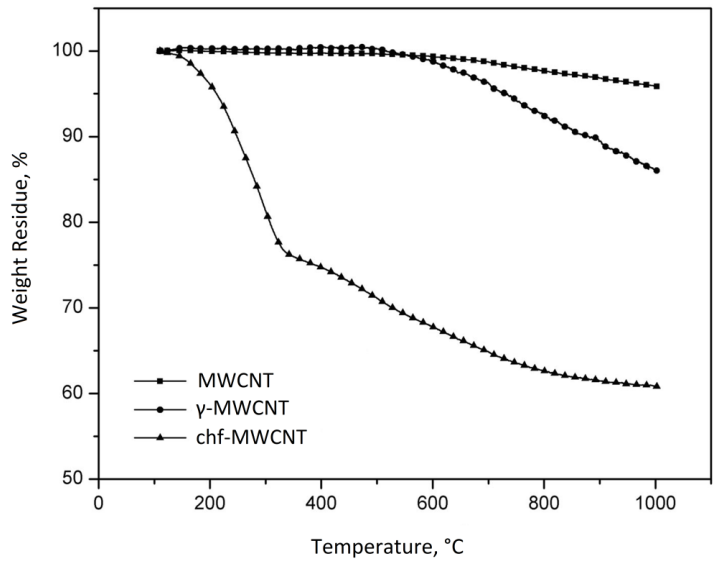

Fig. 3. TG weight loss curves of pristine, irradiation (γ-MWCNT) and chemically functionalized (chf-MWCNT) carbon nanotubes

Also, from Figure 3 it can be noticed that chf-MWCNTs exhibited a 20 % mass loss at 300 °C, increasing nearly to 38 % at temperatures above 900 °C. This loss is due to degradation of –COOH and –OH groups attached to the sidewall of MWCNTs. Irradiation functionalized nanotubes exhibited the total weight loss of 14 % in the temperature range 25 - 1000 °C (Fig. 3). Comparison of TGA data for chf-MWCNTs and γ-MWCNTs clearly indicates that the chemical treatment provides possibilities to attach more functional groups to the MWCNT surface. TGA results are consistent with the above UV-Vis and FT-IR data.

3. 2. Characterisation of f-MWCNT-PLLA nanocomposites

Figures 4 and 5 show FT-IR spectra of neat PLLA, functionalized MWCNTs and corresponding PLLA based nanocomposites. FT-IR spectrum of f-MWCNT displayed a weak carbonyl (C=O) stretching band at 1708 cm^{-1} (Fig. 2).

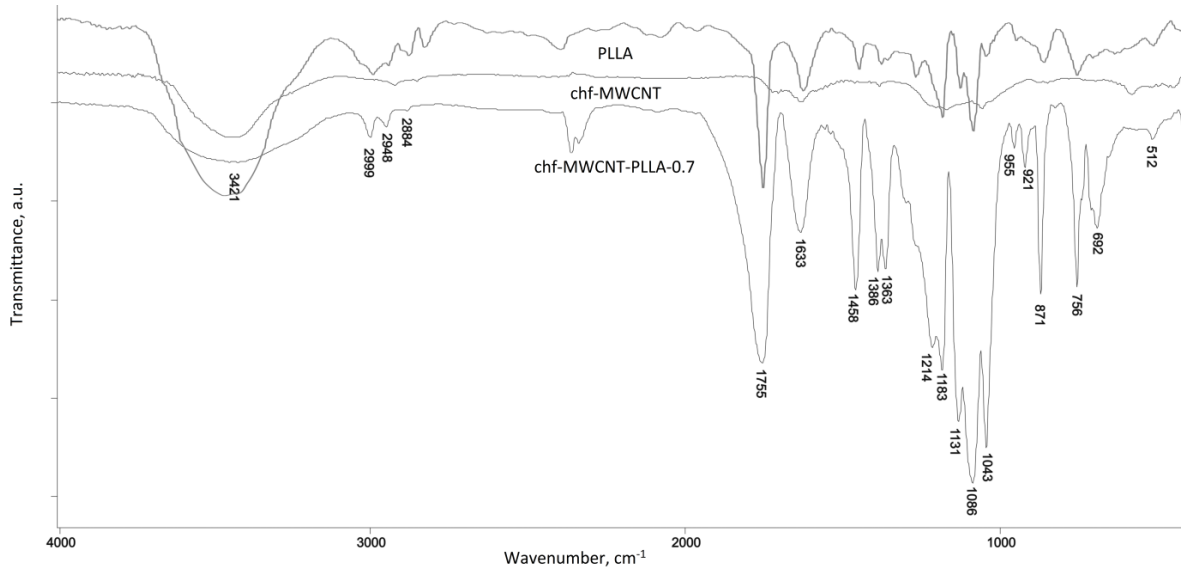

Fig. 4. FT-IR spectra for neat PLLA, chemically functionalized MWCNTs (chf-MWCNT) and PLLA based nanocomposite with 0.7 wt% chemically functionalized MWCNTs (chf-MWCNT-PLLA-0.7)

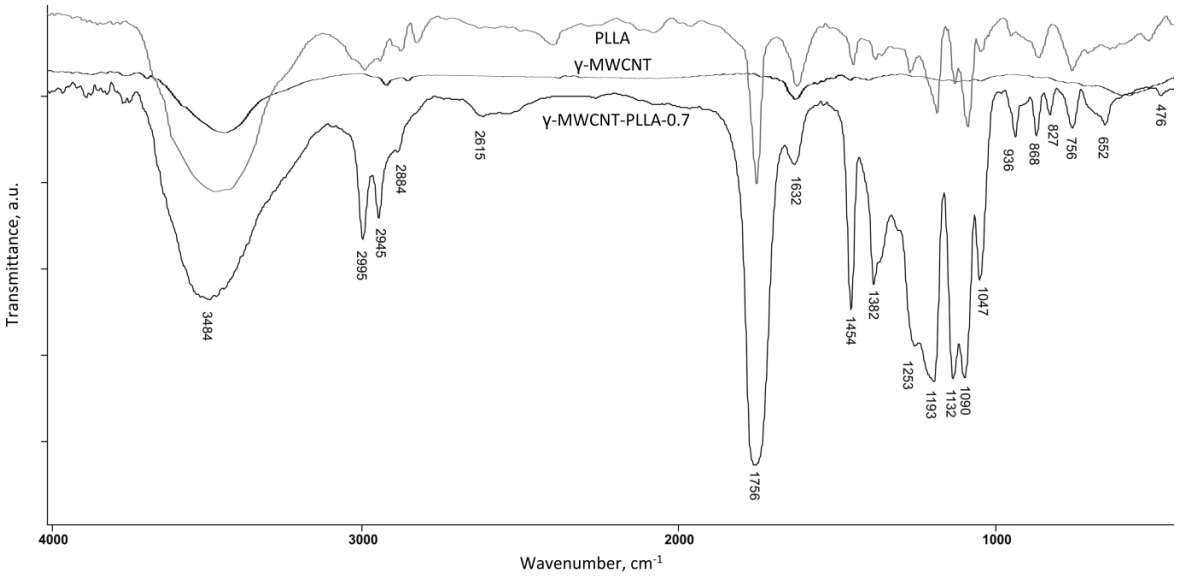

Fig. 5. FT-IR spectra for neat PLLA, irradiation functionalized MWCNTs (γ-MWCNT) and PLLA based nanocomposite with 0.7 wt% irradiation functionalized MWCNTs (γ-MWCNT-PLLA-0.7)

For PLLA composites with f-MWCNTs a more intense C=O stretching band appeared at 1755 cm^{-1} (sample chf-MWCNT-PLLA-0.7) and 1756 cm^{-1} (sample γ-MWCNT-PLLA-0.7). The difference in C=O stretching band positions

between f-MWCNTs and f-MWCNT-PLLA composites is attributed to the fact that the band at 1708 cm^{-1} of f-MWCNTs is due to carboxylic acid groups while the bands at 1755 and 1756 cm^{-1} of f-MWCNT-PLLA composites are originating from the ester groups of grafted PLA chains. In the spectra of the obtained composites a broad absorption band of the hydroxyl (OH) stretching vibrations is present between 3220 and 3590 cm^{-1}. Asymmetrical valence vibrations of C–O–C of the aliphatic polymer chain were shifted to 1183 cm^{-1} and 1193 cm^{-1}, and symmetrical valence vibrations of C–O–C of the aliphatic chain to 1086 and 1090 cm^{-1}, for chf-MWCNT-PLLA-0.7 and γ-MWCNT-PLLA-0.7 composites, respectively, as compared to the bands at 1267 and 1099 cm^{-1} reported for the monomer L-lactide spectrum [37]. FT-IR spectroscopy confirmed successful polymerisation of lactide from the surface of chemically and irradiation functionalized MWCNTs.

Results of DSC analysis of synthesized materials are summarized in Table 2 and Figures 6 and 7. Glass transition temperature (T_g) of the composites is associated to a cooperative motion of polymer chain segments, which may be hindered by the polymer-filler interaction. Therefore, as expected, synthesized f-MWCNT-PLLA composites exhibited higher glass transition temperatures than the PLLA homopolymer (Table 2, Fig. 7). The increase in T_g for f-MWCNT-PLLA nanocomposites is due to the fact that during the *in situ* polymerisation functional groups of f-MWCNT act as initial species for lactide ring-opening polymerisation. These strong bonds, formed between PLA chains and MWCNTs surfaces, are able to hinder the motion of the polymer chains. The T_g values increased with increasing the MWCNTs content in all synthesized samples. Addition of only 2.1 wt% of chf-MWCNTs increased the T_g value up to 18 °C. It was found that changes in T_g for chf-MWCNT-PLLA nanocomposites were more significant than those for γ-MWCNT-PLLA. This finding is attributed to the higher degree of functionalization of chf-MWCNTs, which led to formation of more chemical bonds with PLA chains. In addition, these bonds are stronger than the secondary bonds formed between PLA chains and unmodified MWCNT surfaces and therefore are able to hinder the motion of polymer chains.

Table 2 *Thermal properties of synthesized materials determined by DSC and TGA methods*

Sample name	T_g / °C	T_m / °C	ΔH_m / J g^{-1}	X_c / %	T_{ons} / °C	$T_{10\%}$ / °C
PLLA	47.61	128.58	39.49	42.46	227.40	234.59
chf-MWCNT-PLLA-0.7	52.27	136.60	51.39	55.65	335.70	351.47
chf-MWCNT-PLLA-1.6	54.83	138.64	58.95	64.42	340.70	360.34
chf-MWCNT-PLLA-2.1	65.82	157.81	60.73	66.70	342.03	351.21
γ-MWCNT-PLLA-0.7	52.82	143.84	31.46	34.07	250.20	254.64
γ-MWCNT-PLLA-1.6	53.78	148.01	45.49	49.71	267.40	283.35
γ-MWCNT-PLLA-2.1	60.99	155.39	55.31	60.75	269.10	287.26

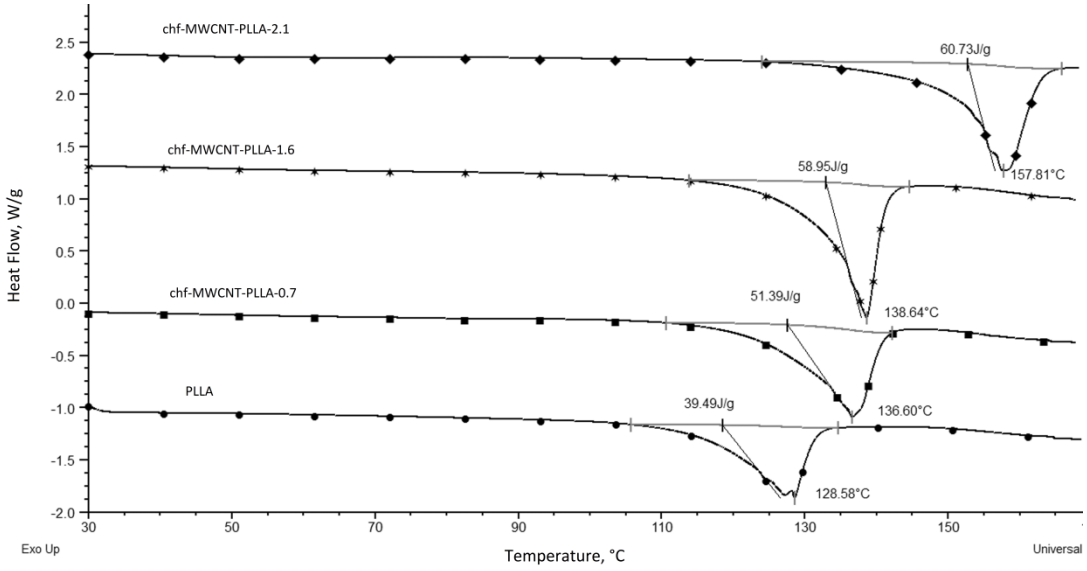

Fig. 6. DSC thermograms of neat PLLA and PLLA based nanocomposites obtained with chemically functionalized carbon nanotubes (chf-MWCNT-PLLA)

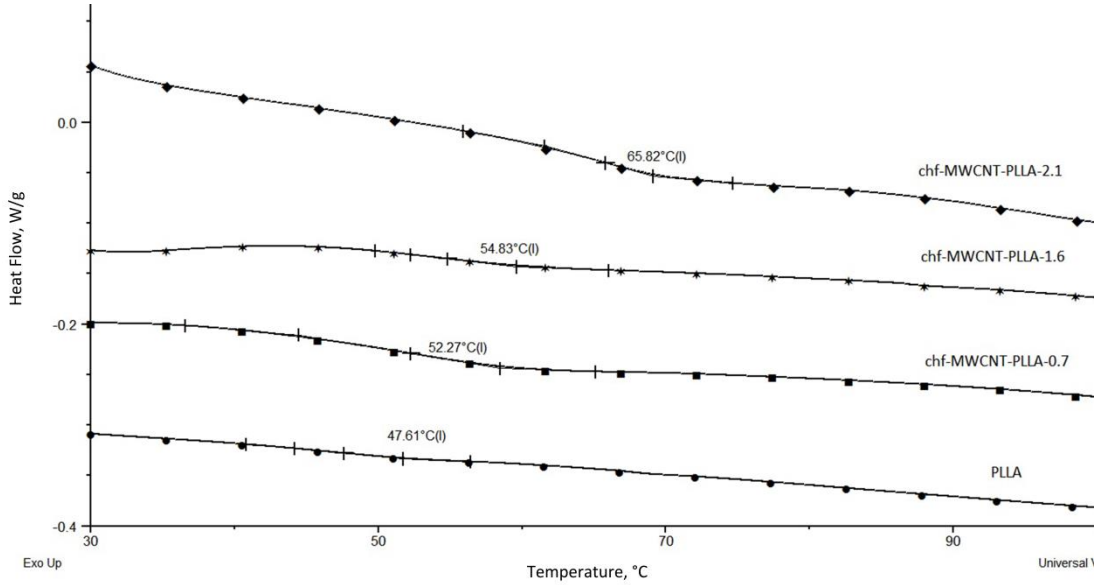

Fig. 7. T_g *values for neat PLLA and PLLA based nanocomposites obtained with chemically functionalized carbon nanotubes (chf-MWCNT-PLLA) (obtained from DSC curves)*

As referenced in literature, MWCNTs can serve as nucleating agents and they facilitate crystallization of PLLA [38]. From the results shown in Table 2 it can be noticed that the crystallization degree (X_c) increased with the increase in the MWCNT content in all nanocomposites, which was expected in relation to the nucleating effect of MWCNTs. It is important to point out that the highest increase in the crystallization degree was detected in composites with chf-MWCNTs, which is a consequence of PLLA crystal shape, and that is also confirmed by AFM measurements.

The melting temperatures (T_m) increased markedly with increasing the content of functionalized MWCNTs in the obtained nanocomposites (Table 2). DSC thermograms of the neat PLLA sample and PLLA based nanocomposites obtained with chemically functionalized carbon nanotubes are shown in Figure 6. The registered increase of Tm is probably the result of the polymer chain arrangement, which became more effective due to the high surface energy of MWCNTs that led to good adhesion to PLLA and enfolding of polymer chains around the MWCNTs, which is also confirmed by SEM and TEM results. The melt enthalpy (ΔH_m) of neat PLLA was 39.49 J g^{-1} and increased with the increase in the content of f-MWCNTs. The value of melt enthalpy increased due to the addition of carbon nanotubes which caused ordered structures of the system. This is also confirmed by the values of the crystallization degree (Table 2).

TGA was used to determine the effect of the f-MWCNT content on thermal stability of nanocomposites, and the results are presented in Figure 8 and Table 2. Thermal stability increased with the increase in f-MWCNTs contents in all prepared nanocomposites. Rise of the initial degradation temperature (T_{ons}) with the increase in f-MWCNTs contents was caused by intensification of chemical bonding between the PLLA matrix and f-MWCNTs and movement obstruction of polymer segments. Decomposition of the chf-MWCNT-PLLA-1.6 sample started at a higher temperature as compared to the γ-MWCNT-PLLA-1.6 sample (Fig. 8). This is a result of functionalization different degrees and interfacial forces in the two nanocomposites. Higher thermal stability of nanocomposite samples prepared with chemically functionalized carbon nanotubes is in accordance with the obtained thermal stability data for f-MWCNTs.

According to TGA measurements, the increase in T_{ons} is about 22 and 108 °C for 0.7 wt% loading of γ-MWCNTs and chf-MWCNTs, respectively. Therefore, TGA results demonstrate that incorporation of a small quantity of f-MWCNT can significantly improve the thermal stability of the f-MWCNT-PLLA composites. Further increase in the f-MWCNTs content had not such a strong effect on T_{ons} values.

Atomic force microscopy studies were used to analyse uniformity of filler dispersions as well as to characterize surface morphology and roughness of f-MWCNT-PLLA composites. Figure 9 shows representative AFM surface topology images of the synthesized samples. The height image and 3D topography of neat PLLA clearly show a smooth surface with a small domain of crystalline phases on the surface (bright dots). The average crystal size was 300 nm, while it

increased with addition of MWCNTs in the PLLA matrix. The nanocomposites had different crystalline structures, more irregular shapes and rougher surfaces in comparison to those found for the neat PLLA sample. Topology features are dependent on the applied carbon nanotube functionalization techniques. Addition of chf-MWCNTs resulted in an ordered crystal domain (Fig. 9b). In the nanocomposite with these MWCNTs, single PLLA covered nanotubes were observed at the surface. Addition of 1.6 wt% γ-MWCNTs significantly increased the diameter of the crystalline phase to 4.1 μm by decreasing the number of domains (Fig. 9c). Due to a lower degree of functionalization, irradiated carbon nanotubes possess lower initial points for the growth of PLLA chains resulting in a higher molecular mass of the obtained polymer, as compared to that in the chf-MWCNT-PLLA composite. For this reason, γ-MWCNT-PLLA composites had lozenge structures.

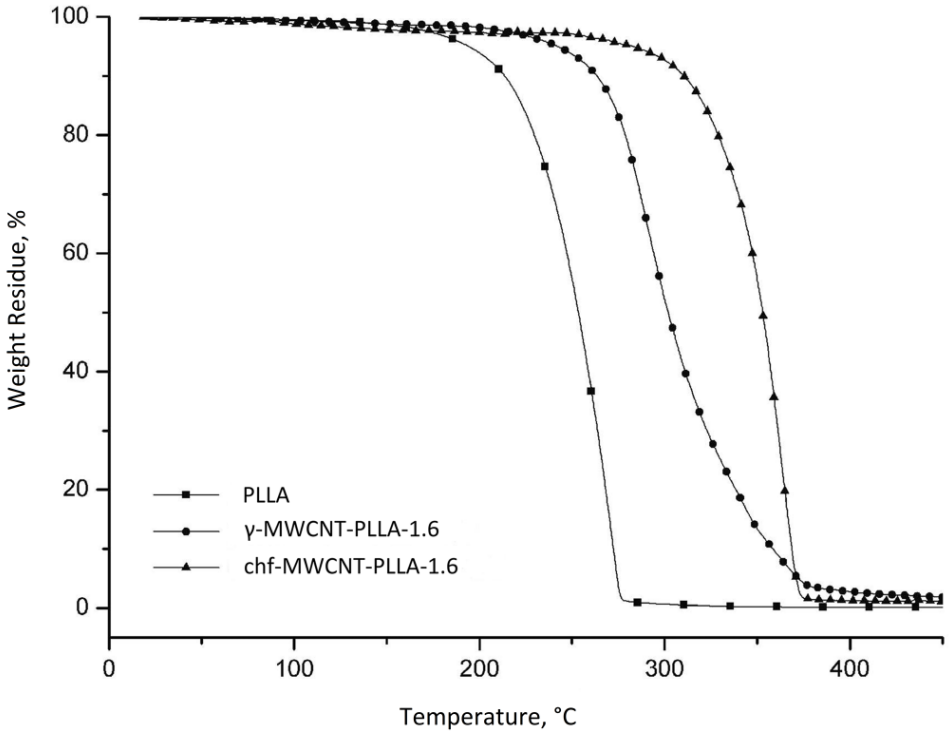

Fig. 8. Weight loss curves obtained by TGA for neat PLLA and PLLA based nanocomposites with 1.6 wt% irradiated (γ-MWCNT-PLLA-1.6) and chemically (chf-MWCNT-PLLA-1.6) functionalized MWCNTs

Scanning electron microscopy was used to study topography and fractured surfaces of f-MWCNT-PLLA nanocomposites. SEM analysis confirmed that in f-MWCNT-PLLA composites the nanotubes appeared embedded into the PLLA matrix (Fig. 10). A higher magnification demonstrates that chf-MWCNTs were completely coated with a PLLA layer resulting in a diameter of ~30 nm, which was significantly larger than that of pristine MWCNTs of 13 nm. This finding suggests strong interactions between f-MWCNTs and grafted PLLA chains. The individual tubes were obviously separated from each other due to the PLLA coating and such "rods" were glued together (Fig. 10a). This indicates that the lactide ring-opening polymerisation reaction took place over the whole surface of functionalized multi-walled carbon nanotubes. Fractured surfaces of the obtained nanocomposites were characterized by SEM as shown in Figure 10b. The γ-MWCNT-PLLA-2.1 nanocomposite displayed relatively smooth fracture surfaces without visible nanotubes pulled out from the PLLA matrix. The fracture surface shows a comb like structure which demonstrates that PLLA chains were chemically bonded to MWCNT surfaces so that the applied strain caused pulling off the PLLA coated MWCNT thread.

Dispersion of f-MWCNTs in the PLLA matrix was evaluated by transmission electron microscopy. The TEM image of the obtained γ-MWCNT-PLLA-2.1 nanocomposite confirmed that functionalized MWCNTs were well dispersed in the polymer (Fig. 11). Good dispersion of MWCNTs also suggests that the used functionalization techniques were appropriate for synthesis of PLLA based nanocomposite materials.

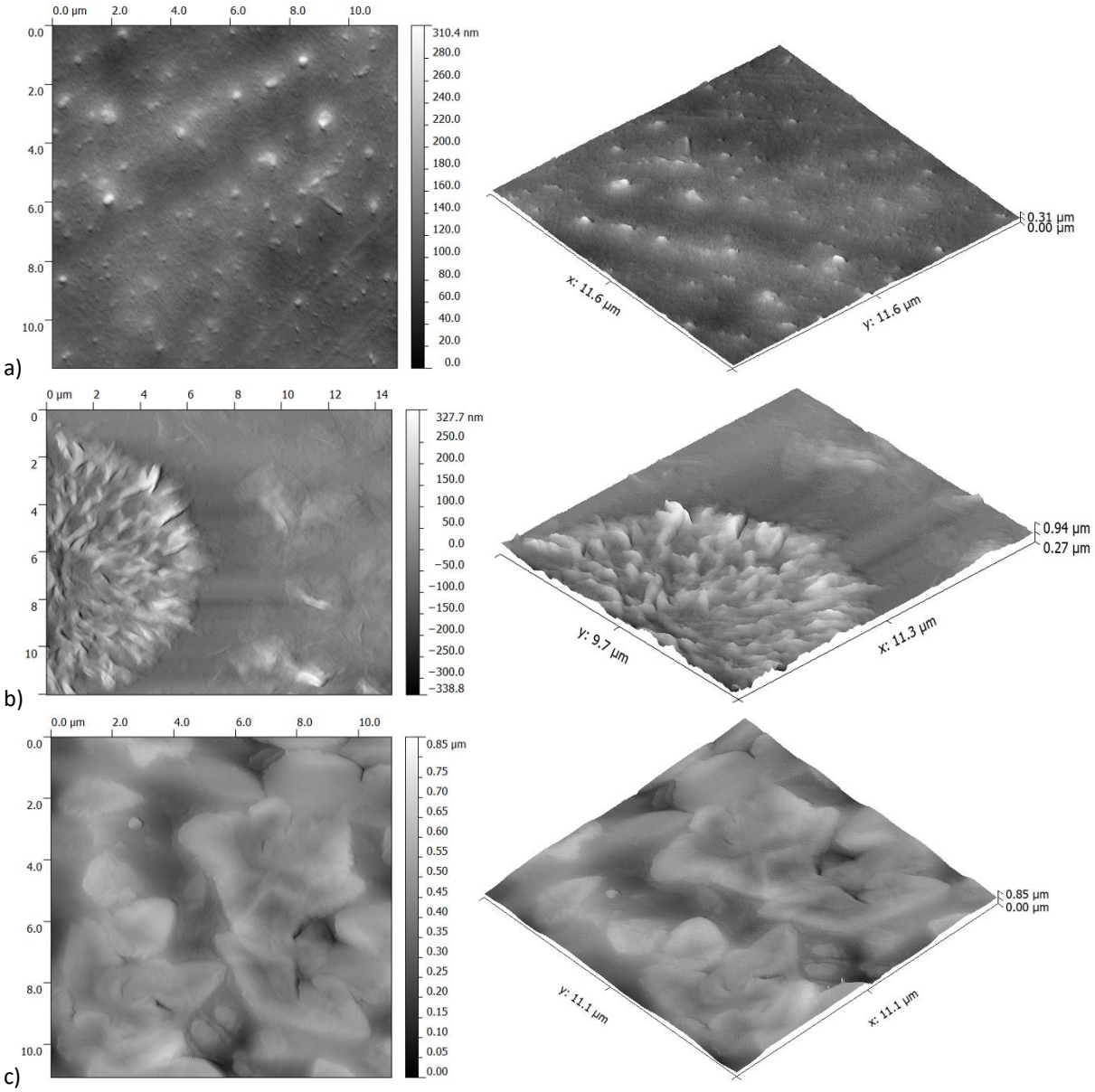

Fig. 9. AFM images of: a) neat PLLA sample, b) PLLA based nanocomposite with 1.6 wt% chemically functionalized MWCNTs (chf-MWCNT-PLLA-1.6), c) PLLA based nanocomposite with 1.6 wt% MWCNTs (γ-MWCNT-PLLA-1.6)

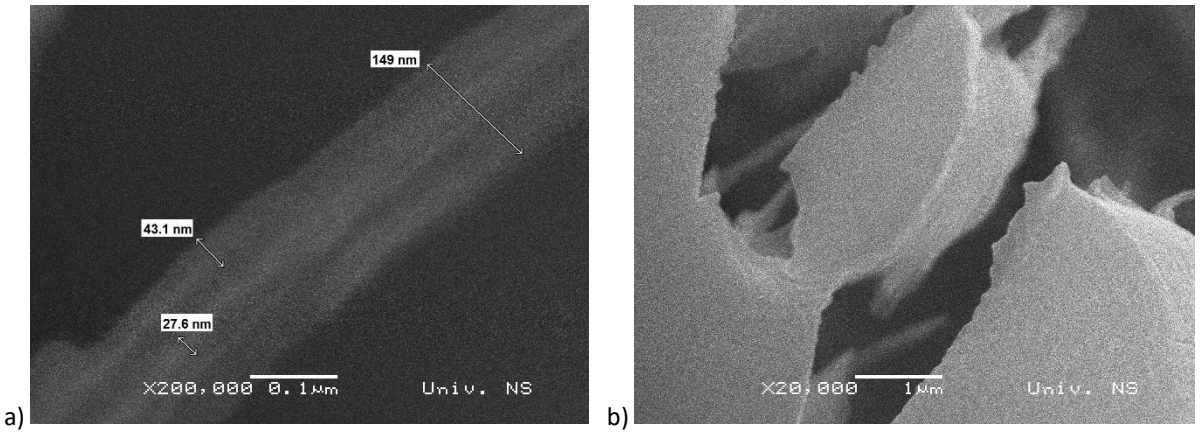

Fig. 10. SEM images of PLLA coated carbon nanotubes (chf-MWCNT-PLLA-2.1), a) and fractured surface of PLLA based nanocomposite with MWCNTs (γ-MWCNT-PLLA-2.1), b)

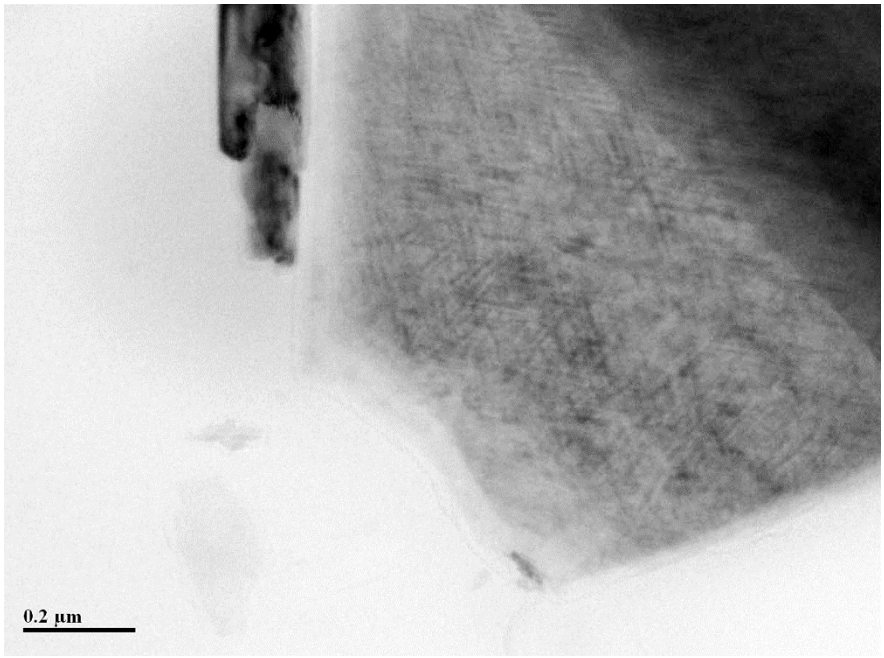

Fig. 11. TEM image of functionalized MWCNTs in the PLLA matrix in the γ-MWCNT-PLLA-2.1 sample

Addition of carbon nanotubes into PLLA can induce electrical conductivity along with enhancement of other beneficial properties of the obtained nanocomposites. The minimum amount of filler required to form a conductive network within a polymer is called a percolation threshold. Percolation threshold should be as low as possible in order to keep the processing simple and the cost low. In this study, a four-point probe was used to measure the sheet resistivity of obtained nanocomposites. The measurements were repeated five times to obtain the averaged resistivity of each sample and the results are presented in Table 3. According to literature data, the sheet resistivity of neat PLLA is 1.2×10^{12} Ω / sq, which confirms its insulating nature [39]. Upon the conductive nanofillers loading, the resistivities were dramatically increased as compared to that of pure PLLA matrix. Sheet resistivity of the obtained PLLA based composites with 0.7 wt% of f-MWCNT was around 105 Ω / sq. This indicates that the conductive path in the nanocomposite was formed and that the electrical conduction path formed by carbon nanotubes in the PLLA matrix reached the percolation threshold. With the further increase in the MWCNT concentration, measured sheet resistivities slightly increased without any significant differences. This phenomenon indicated that the percolation threshold for the electrical conductivity of the nanocomposites was lower than 0.7 wt%. The formation of the percolation threshold was mainly attributed to the conductive network constituted by carbon nanotubes. This result can be explained by the fact that MWCNTs were well dispersed in the polymer matrix. The type of functionalization had a negligible influence on the conductance value, since similar results were obtained for both series of nanocomposites that is chf-MWCNT and γ-MWCNT.

Table 3. Sheet resistivity values of a neat PLLA sample and PLLA based nanocomposites with irradiated and chemically functionalized MWCNTs

Sample name	Sheet resistance, Ω / sq
PLLA	$1.2\text{x}10^{12}$
chf-MWCNT-PLLA-0.7	104.65
chf-MWCNT-PLLA-1.6	118.84
chf-MWCNT-PLLA-2.1	120.25
γ-MWCNT-PLLA-0.7	105.14
γ-MWCNT-PLLA-1.6	116.06
γ-MWCNT-PLLA-2.1	120.39

4. CONCLUSIONS

In this study two approaches were applied for preparation of covalently functionalized multi-walled carbon nanotubes, by the oxidation reaction (with strong acids) and by using high energy gamma irradiation. UV-Vis and FT-IR spectroscopy confirmed successful covalent functionalization of MWCNTs and the presence of –COOH and –OH groups on the nanotube surfaces. To investigate the influence of differently functionalized MWCNTs on the properties of prepared PLLA bionanocomposites, a series of f-MWCNT-PLLA with different nanotube contents were synthesized via ring-opening polymerisation of L-lactide. FT-IR analysis confirmed that this reaction is possible to perform from the surface of functionalized MWCNTs. Even a rather low content of chemically and irradiation functionalized carbon nanotubes had significant influences on thermal properties of the resulting PLLA composites. Therefore, ring-opening polymerisation of lactide in the presence of differently functionalized MWCNTs allows fine-tuning of thermal properties for this very important biopolymer. Incorporation of nanotubes in the PLLA matrix resulted in better ordering of the polymer as assessed from differences in ΔH_m values. The degradation onset temperature for chf-MWCNT-PLLA nanocomposites (above 335 °C), was higher than that for γ-MWCNT-PLLA nanocomposites (above 250 °C), and much higher than the value determined for the neat PLLA (at 227 °C). SEM and TEM analyses indicated that PLLA layers uniformly covered the surface of MWCNTs. Sheet resistivities of f-MWCNT-PLLA nanocomposites indicated that the conductivity percolation was achieved, and that the type of MWCNTs functionalization had a negligible influence on the conductance value. The incorporation of multi-walled carbon nanotubes in the PLLA matrix, which is biodegradable, biocompatible and derived from renewable resources, allowed design of material that possess new functionalities. The properties of this material could be controlled by adjusting the amount of MWCNTs and choosing its type of functionalization, which may be of great interest for its practical applications.

Acknowledgements: *Authors wish to express their gratitude to the Ministry of Education, Science and Technological Development of the Republic of Serbia (Projects III 45022 and III 45020) for financial support.*

REFERENCES

[1] Iijima S. Helical microtubules of graphitic carbon. *Nature*. 1991;354(6348):56-58.
[2] Gupta TK, Kumar S. Fabrication of Carbon Nanotube/Polymer Nanocomposites. *Carbon Nanotub Polym*. January 2018:61-81.
[3] Li H, Zare Y, Rhee KY. The percolation threshold for tensile strength of polymer/CNT nanocomposites assuming filler network and interphase regions. *Mater Chem Phys*. 2018;207:76-83.
[4] Yoon JT, Lee SC, Jeong YG. Effects of grafted chain length on mechanical and electrical properties of nanocomposites containing polylactide-grafted carbon nanotubes. *Compos Sci Technol*. 2010;70(5):776-782.
[5] Choudhary V, Gupt A. Polymer/Carbon Nanotube Nanocomposites. In: *Carbon Nanotubes - Polymer Nanocomposites*. InTech; 2011.
[6] Xiefei Zhang, T. V. Sreekumar, Tao Liu A, Kumar S. Properties and Structure of Nitric Acid Oxidized Single Wall Carbon Nanotube Films. *J Phys Chem B*. 2004;108(42):16435–16440.
[7] Liu, Rinzler, Dai, Hafner, Bradley, Boul, Lu, Iverson, Shelimov, Huffman, Rodriguez-Macias, Shon, Lee, Colbert, Smalley. Fullerene pipes. *Science*. 1998;280(5367):1253-6.
[8] Kleut D, Jovanović S, Marković Z, Kepić D, Tošić D, Romčević N, Marinović-Cincović M, Dramićanin M, Holclajtner-Antunović I, Pavlović V, Dražić G, Milosavljević M, Todorović Marković B. Comparison of structural properties of pristine and gamma irradiated single-wall carbon nanotubes: Effects of medium and irradiation dose. *Mater Charact*. 2012;72:37-45.
[9] Datsyuk V, Kalyva M, Papagelis K, Parthenios J, Tasis D, Siokou A, Kallitsis I, Galiotis C. Chemical oxidation of multiwalled carbon nanotubes. *Carbon N Y*. 2008;46(6):833-840.
[10] Hamon MA, Chen J, Hu H, Chen Y, Itkis ME, Rao AM, Eklund PC, Haddon RC. Dissolution of Single-Walled Carbon Nanotubes. *Adv Mater*. 1999;11(10):834-840.
[11] Chen J, Hamon MA, Hu H, Chen Y, Rao AM, Eklund PC, Haddon RC. Solution properties of single-walled carbon nanotubes. *Science*. 1998;282(5386):95-8.
[12] Baek J-B, Lyons CB, Tan L-S. Grafting of Vapor-Grown Carbon Nanofibers via in-Situ Polycondensation of 3-Phenoxybenzoic Acid in Poly(phosphoric acid). *Macromolecules*. 2004;37(22):8278–8285.
[13] Jin Z, Sun X, Xu G, Goh SH, Ji W. Nonlinear optical properties of some polymer/multi-walled carbon nanotube composites. *Chem Phys Lett*. 2000;318(6):505-510.
[14] Riggs JE, Guo Z, Carroll DL, Sun Y-P. Strong Luminescence of Solubilized Carbon Nanotubes. *J Am Chem Soc*. 2000;122(24):5879-5880.

[15] Lin Y, Zhou B, Shiral Fernando KA, Liu P, Allard LF, Sun Y-P. Polymeric Carbon Nanocomposites from Carbon Nanotubes Functionalized with Matrix Polymer. *Macromolecules*. 2003;36(19):7199-7204.

[16] Yang M, Gao Y, Li H, Adronov A. Functionalization of multiwalled carbon nanotubes with polyamide 6 by anionic ring-opening polymerization. *Carbon N Y*. 2007;45(12):2327-2333.

[17] Kong H, Luo P, Gao C, Yan D. Polyelectrolyte-functionalized multiwalled carbon nanotubes: preparation, characterization and layer-by-layer self-assembly. *Polymer (Guildf)*. 2005;46(8):2472-2485.

[18] Kong H, Li W, Gao C, Yan D, Jin Y, Walton DRM, Kroto HW. Poly(N-isopropylacrylamide)-Coated Carbon Nanotubes: Temperature-Sensitive Molecular Nanohybrids in Water. *Macromolecules*. 2004;37(18):6683–6686.

[19] Qin S, Qin D, Ford WT, Herrera JE, Resasco Daniel E. Grafting of Poly(4-vinylpyridine) to Single-Walled Carbon Nanotubes and Assembly of Multilayer Films. *Macromolecules*. 2004;37(26):9963–9967.

[20] Baskaran D, Mays JW, Bratcher MS. Polymer-Grafted Multiwalled Carbon Nanotubes through Surface-Initiated Polymerization. *Angew Chemie Int Ed*. 2004;43(16):2138-2142.

[21] Seligra PG, Nuevo F, Lamanna M, Famá L. Covalent grafting of carbon nanotubes to PLA in order to improve compatibility. *Compos Part B Eng*. 2013;46:61-68.

[22] Sun J, Shen J, Chen S, Cooper M, Fu H, Wu D, Yang Z, Sun J, Shen J, Chen S, Cooper MA, Fu H, Wu D, Yang Z. Nanofiller Reinforced Biodegradable PLA/PHA Composites: Current Status and Future Trends. *Polymers (Basel)*. 2018;10(5):505.

[23] Kaseem M, Hamad K, Deri F, Ko YG. A review on recent researches on polylactic acid/carbon nanotube composites. *Polym Bull*. 2017;74(7):2921-2937.

[24] Seligra PG, Lamanna M, Famá L. Promising PLA-functionalized MWCNT composites to use in nanotechnology. *Polym Compos*. 2016;37(10):3066-3072.

[25] Abozar Akbari, Mainak Majumder AT. Polylactic Acid (PLA) Carbon Nanotube Nanocomposites. In: Al. JKP et, ed. *Handbook of Polymer Nanocomposites. Processing, Performance and Application – Volume B: Carbon Nanotube Based Polymer Composites*. Springer-Verlag Berlin Heidelberg; 2015:283-297.

[26] Gonçalves C, Gonçalves I, Magalhães F, Pinto A, Gonçalves C, Gonçalves IC, Magalhães FD, Pinto AM. Poly(lactic acid) Composites Containing Carbon-Based Nanomaterials: A Review. *Polymers (Basel)*. 2017;9(12):269.

[27] Kim H, Abdala AA, Macosko CW. Graphene/Polymer Nanocomposites. *Macromolecules*. 2010;43(16):6515-6530.

[28] Brzeziński M, Biela T. Polylactide nanocomposites with functionalized carbon nanotubes and their stereocomplexes: A focused review. *Mater Lett*. 2014;121:244-250.

[29] Jovanovic S, Markovic Z, Kleut D, Kepic D, Tosic D, Todorovic-Markovic B, Holclajtner-Antunovic I, Marinovic-Cincovic M. Covalent modification of single wall carbon nanotubes upon gamma irradiation in aqueous media. *Hem Ind*. 2011;65(5):479-487.

[30] Marković VM, Eymery R, Yuan HC. A new approach of 60Co plant design for introduction of radiation sterilization in developing countries. *Radiat Phys Chem*. 1977;9(4-6):625-631.

[31] Ke T, Sun X. Effects of Moisture Content and Heat Treatment on the Physical Properties of Starch and Poly(lactic acid) Blends. *J Appl Polym Sci*. 2001;81(12):3069-3082.

[32] Blythe AR. Electrical resistivity measurements of polymer materials. *Polym Test*. 1984;4(2-4):195-209.

[33] Qian Z, Wang C, Du G, Zhou J, Chen C, Ma J, Chen J, Feng H. Multicolour fluorescent graphene oxide by cutting carbon nanotubes upon oxidation. *CrystEngComm*. 2012;14(15):4976.

[34] Bafandeh N, Larijani MM, Shafiekhani A, Hantehzadeh MR, Sheikh N. Effects of Contents of Multiwall Carbon Nanotubes in Polyaniline Films on Optical and Electrical Properties of Polyaniline. *Chinese Phys Lett*. 2016;33(11):117801.

[35] Bhatia R, Kumar L. Functionalized carbon nanotube doping of P3HT:PCBM photovoltaic devices for enhancing short circuit current and efficiency. *J Saudi Chem Soc*. 2017;21(3):366-376.

[36] Wepasnick KA, Smith BA, Bitter JL, Howard Fairbrother D. Chemical and structural characterization of carbon nanotube surfaces. *Anal Bioanal Chem*. 2010;396(3):1003-1014.

[37] Ristić IS, Tanasić L, Nikolić LB, Cakić SM, Ilić OZ, Radičević RŽ, Budinski-Simendić JK. The Properties of Poly(l-Lactide) Prepared by Different Synthesis Procedure. *J Polym Environ*. 2011;19(2):419-430.

[38] Xu H-S, Dai XJ, Lamb PR, Li Z-M. Poly(L-lactide) crystallization induced by multiwall carbon nanotubes at very low loading. *J Polym Sci Part B Polym Phys*. 2009;47(23):2341-2352.

[39] Yoon JT, Jeong G, Lee SC, Min BG. Influences of poly(lactic acid)-grafted carbon nanotube on thermal, mechanical, and electrical properties of poly(lactic acid). *Polym Adv Technol*. 2009;20(7):631-638.

SAŽETAK

Uticaj različitih metoda funkcionalizacije višeslojnih ugljeničnih nanocevi na svojstva nanokompozita na osnovu poli(L-laktida)

Nevena Vukić[1], Ivan S Ristić[1], Milena Marinović-Cincović[2], Radmila Radičević[1], Branka Pilić[1], Suzana Cakić[3] i Jaroslava Budinski-Simendić[1]

[1]*Univerzitet u Novom Sadu, Tehnološki fakultet Novi Sad, Novi Sad, Srbija*
[2]*Institut za nuklearne nauke Vinča, Univerzitet u Beogradu, Srbija*
[3]*Univerzitet u Nišu, Tehnološki fakultet, Leskovac, Srbija*

(Naučni rad)

U radu je prikazan uticaj vrste funkcionalizacije ugljeničnih nanocevi na svojstva nanokompozitnih materijala baziranih na poli(L-laktidu). U tu svrhu izvršena je modifikacija površine višeslojnih ugljeničnih nanocevi hemijskom metodom (oksidacijom kiselinama) i ozračivanjem. Prisustvo odgovarajućih funkcionalnih grupa na površini ugljeničnih nanocevi, nakon njihove modifikacije, utvrđeno je na osnovu rezultata UV-vidljive spektroskopije, infracrvene spektroskopije sa Furijeovom transformacijom (engl. *Fourier-transform infrared* - FT-IR) i termogravimetrijske analize (TGA). Serije bionanokompozita na bazi poli(L-laktida) sa različitim udelima funkcionalizovanih višeslojnih ugljeničnih nanocevi (0,7; 1,6; 2,1 mas. %), sintetisane su polimerizacijom L-laktida otvaranjem prstena u rastvoru. FT-IR analizom potvrđeno je da je ovaj tip polimerizacije (kalemljenje), u kontrolisanim uslovima, moguće izvesti sa površine funkcionalizovanih ugljeničnih nanocevi. Na osnovu primene metode diferencijalne skenirajuće kalorimetrije zaključeno je da vrlo mali udeli hemijski i radijaciono funkcionalizovanih nanocevi imaju značajan uticaj na termička svojstva pripremljenih nanokompozita, povećavajući vrednosti temperature topljenja i temperature prelaska u staklasto stanje dobijenih nanokompozita. TGA analizom ustanovljeno je da je temperatura degradacije kompozita sa hemijski modifikovanim ugljeničnim nanocevima, mnogo viša od temperature degradacije poli(L-laktida), kao i kompozita sa radijaciono funkcionalizovanim nanocevima. Morfološke studije skenirajućim elektronskim mikroskopom (SEM) i transmisionim elektronskim mikroskopom (TEM) pokazale su da poli(L-laktid) prekriva površinu funkcionalizovanih nanocevi i razdvaja ih omogućavajući na taj način dobru disperziju nanocevi unutar polimerne matrice. Dobra disperzija ugljeničnih nanocevi u poli(laktidu) omogućila je električnu provodljivost sintetisanih materijala, što je i potvrđeno testom provodljivosti.

Ključne reči: nanokompoziti; funkcionalizacija ugljeničnih nanocevi; poli(L-laktid); termička svojstva